Journal of Natural and Artificial Scientific Systems, 2026, 3(2): 219-237

Green Synthesis and Characterization of Titanium Dioxide (TiO_2) Nanoparticles Using Rice Husk Extract

Mukhtar Saifullahi*, Okunola Oluwole Joshua and Abdullahi Haruna

Received: 04 March 2026/Accepted: 14 June 2026/Published: 24 June 2026

Abstract: *Green synthesis of titanium dioxide (TiO_2) nanoparticles has emerged as an environmentally sustainable alternative to conventional chemical methods because it eliminates the use of hazardous reducing agents and utilizes naturally occurring phytochemicals for nanoparticle formation and stabilization. This study synthesized TiO_2 nanoparticles using aqueous rice husk (Oryza sativa) extract and evaluated their physicochemical properties using ultraviolet-visible (UV–Vis) spectroscopy, Fourier transform infrared (FTIR) spectroscopy, X-ray diffraction (XRD), scanning electron microscopy coupled with energy-dispersive X-ray spectroscopy (SEM–EDX), and X-ray fluorescence (XRF). Rice husk extract was prepared by aqueous extraction and reacted with titanium tetraisopropoxide (TTIP), followed by drying at 110 °C and calcination at 500 °C for 2 h. UV–Vis analysis exhibited a characteristic absorption maximum at 374 nm, corresponding to an estimated optical band gap of 3.32 eV, confirming the formation of nanosized TiO_2. FTIR spectra revealed prominent absorption bands at 3332, 1550, 1274, 1021, 820, and 599 cm^{-1}, assigned to O–H, C–O, O–C–O, Ti–O–Ti, and Ti–O functional groups, demonstrating the participation of rice husk phytochemicals during nanoparticle synthesis and stabilization. XRD analysis showed diffraction peaks at 2θ = 25.39°, 27.50°, 36.16°, 41.26°, 48.05°, 53.92°, 54.37°, 56.64°, and 62.85°, confirming the formation of predominantly anatase TiO_2 with a minor rutile phase. SEM micrographs revealed predominantly spherical, agglomerated nanoparticles with rough and porous surface morphology, while EDX analysis identified titanium as the dominant element with 95.97 at.% and 96.71 wt.%. XRF analysis further confirmed high chemical purity, with TiO_2 constituting 87.09 wt.% of the total oxide composition and only trace quantities of other oxides. The excellent agreement among the UV–Vis, FTIR, XRD, SEM–EDX, and XRF analyses confirms the successful green synthesis of highly crystalline and chemically stable TiO_2 nanoparticles. These nanoparticles possess physicochemical characteristics suitable for photocatalysis, wastewater treatment, environmental remediation, antimicrobial coatings, and other sustainable nanotechnology applications..*

Keywords*: Green synthesis, Characterization, Titanium dioxide nanoparticles, Rice husk*

Mukhtar Saifullahi*
Department of Chemistry, Federal University of Agriculture Zuru, Kebbi State, Nigeria.
Email: Saifullahimukhtar406@gmail.com

Okunola Oluwole Joshua
Department of Chemistry, Federal University Dutsin-Ma, Katsina State, Nigeria.
Email: ookunola@fudutsinma.edu.ng
https://orcid.org/0000-0001-6547-9874

Abdullahi Haruna
Department of Chemistry, Federal University Dutsin-Ma, Katsina State, Nigeria.
Email: habdullahi@fudutsinma.edu.ng
https://orcid.org/0009-0005-7743-2199

1.0 Introduction

Titanium dioxide (TiO_2) nanoparticles have attracted considerable attention because of their remarkable photocatalytic activity, chemical stability, non-toxicity, cost-effectiveness, and excellent optical properties. These characteristics have promoted their application in wastewater treatment, environmental remediation, self-cleaning surfaces, antimicrobial coatings, solar energy conversion, and other advanced technological fields (Mittal *et al*., 2013). Among the three naturally occurring crystalline phases of TiO_2 (anatase, rutile, and brookite), the anatase phase is widely recognized for its superior photocatalytic efficiency owing to its high surface area, enhanced charge separation efficiency, and strong oxidative capability (Aminzai *et al*., 2024). Owing to these exceptional physicochemical properties, TiO_2 nanoparticles have become one of the most extensively investigated semiconductor nanomaterials for environmental and energy-related applications. Their high photocatalytic efficiency, excellent photostability, and resistance to chemical corrosion have made them attractive for wastewater purification, air pollution control, hydrogen generation, antimicrobial coatings, dye degradation, and solar energy conversion. Consequently, there is growing interest in developing environmentally sustainable methods for producing TiO_2 nanoparticles with improved physicochemical properties while minimizing environmental impacts.

TiO_2 has also attracted considerable industrial and scientific interest because of its chemical stability, strong oxidizing ability, low toxicity, and ease of synthesis. These characteristics have facilitated its application in photocatalysis, antimicrobial coatings, degradation of volatile organic compounds, water splitting for hydrogen production, and biomedical applications such as cancer therapy under light irradiation (Chen et al., 2020). These properties underpin its application in photocatalysis, where TiO_2 functions as an efficient antiviral and antibacterial agent, facilitates the degradation of volatile organic compounds, promotes water splitting, and contributes to cancer cell destruction under irradiation (Chen *et al*., 2020). Despite the outstanding properties and numerous applications of TiO_2 nanoparticles, their conventional synthesis methods—including sol-gel, hydrothermal, chemical precipitation, and solvothermal techniques—often require hazardous chemicals, elevated temperatures, and sophisticated instrumentation.

(Al-Mamun *et al*., 2022; Baamer *et al*., 2024). These limitations have stimulated growing interest in green synthesis approaches that utilize biological materials as environmentally benign reducing and stabilizing agents. Green synthesis offers several advantages, including reduced toxicity, lower energy consumption, improved biocompatibility, and sustainable nanoparticle production (Souza *et al*., 2025).

Several biological resources, including bacteria, fungi, algae, and higher plant extracts, have been successfully employed for the green synthesis of TiO_2 nanoparticles (Alcazar *et al*., 2026; Shakeel *et al*., 2025; Syed *et al*., 2026). Among these, plant-mediated synthesis has received the greatest attention because plant extracts are inexpensive, readily available, non-toxic, and rich in bioactive phytochemicals capable of acting simultaneously as reducing, stabilizing, and capping agents (Akpanudo & Olabemiwo, 2024a,b). Previous studies have reported the successful synthesis of TiO_2 nanoparticles using extracts of *Aloe vera*, *Azadirachta indica* (neem), *Moringa oleifera*, green tea, and numerous other plant species with varying physicochemical characteristics depending on the phytochemical composition of the extract ((Awad *et al*., 2025; Pamdey *et al*., 2026; Ragman *et al*., 2026).

Plant-mediated synthesis of nanoparticles has attracted considerable attention because plants contain diverse phytochemicals, including flavonoids, phenolics, alkaloids, tannins, terpenoids, and saponins, which function as natural reducing, stabilizing, and capping agents during nanoparticle formation (Srikar et al., 2016). Among various agricultural residues, rice husk (*Oryza sativa*) represents an abundant, renewable, and low-cost biomass rich in silica, cellulose, hemicellulose, lignin, and polyphenolic compounds. These bioactive constituents facilitate the reduction of titanium precursors while simultaneously enhancing nanoparticle stability. Consequently, rice husk provides an environmentally sustainable alternative for the biosynthesis of TiO_2 nanoparticles while simultaneously promoting agricultural waste valorization. Its flavonoids, terpenoids, phenolics, and essential oils provide strong reducing and capping capabilities that support the eco-friendly formation of TiO_2 nanoparticles with enhanced stability and functional performance (Al-Mamun *et al*., 2022; Baamer *et al*., 2024). Titanium dioxide nanoparticles possess excellent thermal stability, chemical inertness, low toxicity, and high resistance to photochemical degradation, making them environmentally safe and suitable for numerous industrial applications (Ganapathi et al., 2015). These properties have encouraged their use in wastewater treatment, removal of atmospheric pollutants such as nitrogen oxides (NOx), photocatalytic degradation of organic contaminants, antimicrobial coatings, and self-cleaning materials (Sethy et al., 2020).In this work, the synthesis of titanium oxide nanoparticles was carried out because this compound has various applications, among them, the removal of pollutants in water or the photo-degradation of atmospheric pollutants such as nitrogen oxides (NO_x), to mention a few (Sethy *et al*., 2020). Although numerous studies have reported the green synthesis of TiO_2 nanoparticles using various medicinal plants and herbal extracts, comparatively few investigations have explored the use of rice husk, an abundant agricultural waste, as both the reducing and stabilizing agent. Furthermore, comprehensive characterization of rice husk-mediated TiO_2 nanoparticles using complementary analytical techniques remains limited, particularly regarding their physicochemical properties relevant to environmental remediation applications.

Unlike previous studies that employed plant extracts such as *Aloe vera*, neem, and *Moringa oleifera* for the biosynthesis of TiO_2 nanoparticles, the present study utilized rice husk extract, an abundant agricultural waste in northern Nigeria, as both the reducing and stabilizing agent. Therefore, the aim of this study was to synthesize TiO_2 nanoparticles through a green route using rice husk extract and to comprehensively characterize the synthesized nanoparticles using UV–Vis, FTIR, XRD, SEM–EDX, and XRF techniques in order to evaluate their physicochemical properties and potential suitability for environmental remediation applications**.** The findings of this study are expected to contribute to sustainable nanotechnology by demonstrating an environmentally benign approach for converting agricultural waste into value-added nanomaterials. In addition, the study promotes waste valorization, reduces dependence on hazardous chemical synthesis routes, and provides useful baseline information for the future development of low-cost TiO_2 nanoparticles for photocatalytic, water treatment, and environmental remediation applications.The synthesized nanoparticles were comprehensively characterized using UV–Vis, FTIR, XRD, SEM–EDX and XRF to evaluate their physicochemical properties and potential suitability for environmental remediation applications

2.0 Materials and Methods

2.1 Materials

Titanium tetraisopropoxide (TTIP) was used as the titanium precursor for nanoparticle synthesis. All chemicals and reagents used in this study were of analytical grade and were used without further purification. Distilled water was used throughout the experimental procedures.

Rice husk used in this study was collected from Darma Rice Mill, Katsina State, Nigeria**.** The botanical identity of the rice husk was authenticated at the Department of Biological Sciences, Federal University Dutsin-Ma (FUDMA), Katsina State, where it was identified as *Oryza sativa* with Voucher Identification Number FUDMA/PSB/00197**.**
The collected rice husk was thoroughly washed with distilled water to remove dust, soil particles, and other adhering impurities.The washed rice husk was oven-dried at 60 °C for 12 h to remove residual moisture before being ground into a fine powder using a mechanical grinder.Rice husk powder (50 g) was added to 100 mL of distilled water and boiled on a hotplate at 80°C for 30 minutes. The resulting mixture was filtered using Whatman filter paper No. 1 to obtain a clear rice husk extract, which was stored for subsequent use in the nanoparticle synthesis process (Aravind *et al.,* 2021). The filtrate was allowed to cool to room temperature and stored at 4 °C until further use in the nanoparticle synthesis.

2.2 Synthesis of TiO_2 Nanoparticles

For the green synthesis of TiO_2 nanoparticles, 50 mL of titanium tetraisopropoxide (TTIP) was transferred into a clean 250 mL beaker.Twenty millilitres (20 mL) of rice husk extract were added dropwise to the TTIP solution under continuous magnetic stirring at room temperature (25 ± 2 °C). The reaction mixture was continuously stirred for 3 h, during which the colour gradually changed from white to yellowish-grey, indicating the formation of TiO_2 nanoparticles.The reaction mixture was filtered using Whatman No. 1 filter paper, and the recovered nanoparticles were washed three times with distilled water to remove residual precursor and other impurities.The nanoparticles were washed three times with distilled water to remove any unreacted precursors and impurities. The washed nanoparticles was dried at 110 °C for 5 hours. The dried nanoparticles were subsequently calcined in a muffle furnace at 500 °C for 2 h to improve crystallinity and obtain the anatase TiO_2 phase (Aravind et al., 2021).

2.3 Characterization of TiO_2 Nanoparticle

The synthesized TiO_2 nanoparticles were characterized to determine their optical properties, functional groups, crystalline structure, elemental composition, surface morphology, and particle characteristics. Ultraviolet-visible (UV–Vis) spectroscopy was used to evaluate the optical absorption behaviour of the nanoparticles. Fourier transform infrared (FTIR) spectroscopy was employed to identify the functional groups involved in nanoparticle formation and stabilization. X-ray diffraction (XRD) analysis was carried out to determine the crystalline phases and structural properties of the synthesized nanoparticles. The elemental and oxide compositions were determined using energy-dispersive X-ray spectroscopy (EDX) and X-ray fluorescence (XRF), respectively, while scanning electron microscopy (SEM) was used to examine the morphology and surface characteristics of the nanoparticles. The UV–Vis spectra were recorded over the wavelength range of 200–800 nm. FTIR spectra were obtained within the range of 4000–400 cm^{-1}. XRD analysis was performed using Cu-Kα radiation (λ = 1.5406 Å), while SEM–EDX and XRF analyses were conducted according to the operating procedures of the respective instruments.

3.0 Results and Discussions

3.1 Characterization of TiO_2 Nanoparticles (NPs) from Rice Husk

3.1.1 Ultraviolet-visible Analysis

The UV–Vis absorption spectrum of the biosynthesized TiO_2 nanoparticles is presented in Fig. 1. The spectrum exhibits a single, intense, and well-defined absorption band with a maximum absorbance (λ_{max}) at approximately 374 nm, followed by a gradual decrease in absorbance toward the visible region, producing a long absorption tail up to about 1200 nm. The sharp absorption edge and asymmetric spectral profile are characteristic of nanosized TiO_2 particles and indicate efficient electronic excitation from the valence band to the conduction band. The absence of additional absorption peaks suggests that the synthesized material is relatively free from secondary photoactive impurities and possesses good optical purity.

The absorption maximum observed at 374 nm is slightly blue-shifted relative to bulk anatase TiO_2, which typically exhibits an absorption edge around 380 nm. This blue shift is attributed to the quantum confinement effect, whereby a reduction in crystallite size results in an increase in the energy required for electronic excitation. Similar absorption maxima within the range of 371–380 nm have been reported for green-synthesized TiO_2 nanoparticles prepared using plant extracts (Bagheri et al., 2013), confirming that the optical behaviour observed in the present study is consistent with nanoscale anatase TiO_2.

The optical band gap energy (E_{BG}) of the synthesized TiO_2 nanoparticles can be estimated from the absorption maximum using equation 1 (Eddy *et al.*, 2023, 2024)

$$E_{BG} = \frac{hc}{\lambda_{max}} \quad (1)$$

where E_{BG} is the band gap energy (eV) and λ is the absorption wavelength (nm).

Using the absorption maximum of 374 nm, E_{BG}, is obtained. The calculated band gap of 3.32 eV is slightly higher than that of bulk anatase TiO_2 (approximately 3.20 eV), further confirming the nanoscale nature of the synthesized particles. The increase in band gap energy is consistent with the observed blue shift and indicates reduced particle dimensions resulting from the green synthesis route. Band gap values between 3.20 and 3.35 eV have been widely reported for biosynthesized anatase TiO_2 nanoparticles (Bagheri et al., 2013; Aravind et al., 2021).

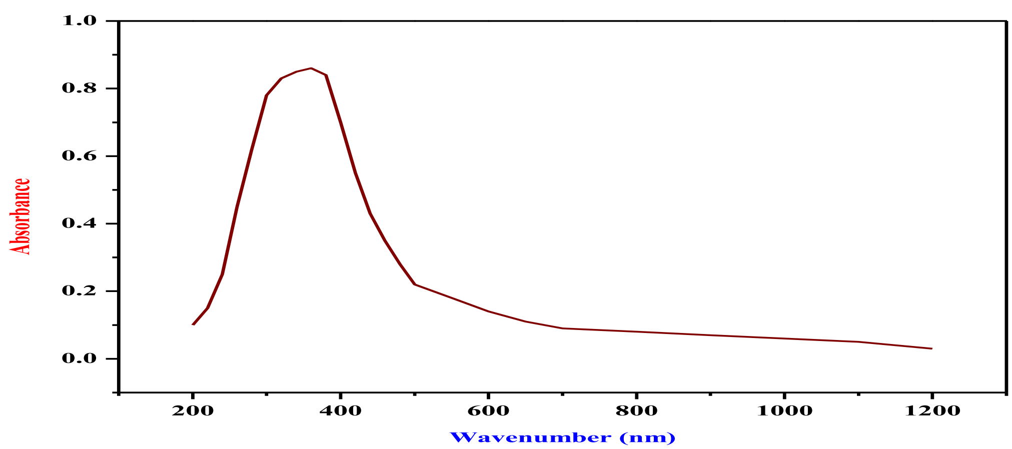

Fig. 1: UV–Visible absorption spectrum of the biosynthesized TiO_2 NPs

The shape of the UV–Vis spectrum also provides important information about the optical quality of the nanoparticles. The steep rise in absorbance near the absorption edge indicates rapid photon absorption and efficient electron transition, whereas the gradual decline in absorbance toward longer wavelengths suggests minimal light scattering and a relatively homogeneous nanoparticle population. The absence of broad secondary absorption bands further indicates that significant impurity phases or surface defect states were not introduced during the biosynthesis process.

The optical properties obtained demonstrate that the rice husk-mediated TiO_2 nanoparticles possess excellent photoresponsive characteristics suitable for ultraviolet-light-driven photocatalytic applications.

A band gap energy of 3.32 eV enables effective generation of electron-hole pairs under UV irradiation, thereby promoting the formation of reactive oxygen species responsible for the degradation of organic contaminants and microbial inactivation. These findings therefore suggest that the biosynthesized TiO_2 nanoparticles have considerable potential for applications in The UV–Vis results also complement the XRD, FTIR, and SEM–EDX analyses, collectively confirming the successful green synthesis of crystalline TiO_2 nanoparticles with desirable optical properties for environmental and photocatalytic applications.

3.1.2 Fourier Transform Infra-Red Analysis

The FTIR spectrum of the biosynthesized TiO_2 nanoparticles is presented in Fig. 2. The spectrum exhibits several characteristic absorption bands distributed between 4000 and 500 cm^{-1}, indicating the presence of surface functional groups originating from the rice husk extract as well as the successful formation of titanium dioxide. The overall spectrum is characterized by a broad absorption band in the high wavenumber region (3000–3500 cm^{-1}) and several distinct peaks in the fingerprint region (<1700 cm^{-1}), which are typical of plant-mediated TiO_2 nanoparticles.

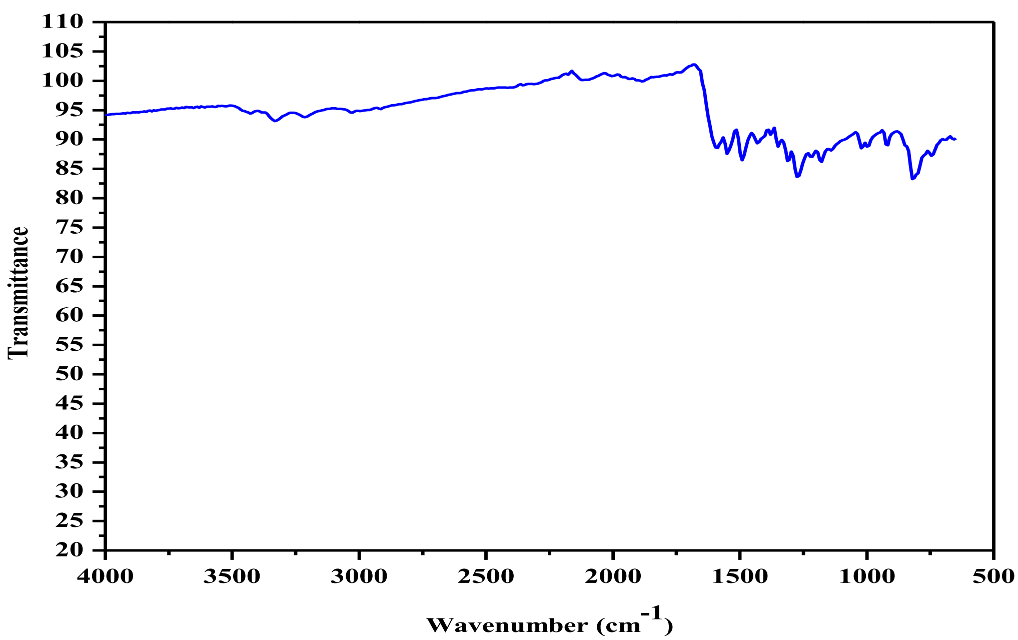

Fig. 2: FTIR of the synthesized nanoparticles

The broad absorption band centered at 3332 cm^{-1} corresponds to the O–H stretching vibration of hydroxyl groups associated with adsorbed water molecules and phenolic compounds present in the rice husk extract. The broadness of this band suggests extensive intermolecular hydrogen bonding between hydroxyl-containing phytochemicals and the nanoparticle surface. Hydroxyl groups play an important role during green synthesis by acting as electron donors that reduce titanium ions while simultaneously stabilizing the nanoparticles through surface adsorption. Surface hydroxyl groups are also known to improve photocatalytic efficiency because they serve as active sites for the generation of hydroxyl radicals (•OH) during UV irradiation, thereby enhancing degradation of organic pollutants (Srujana et al., 2022).

A moderately intense absorption band observed at 1550 cm^{-1} is assigned to the O–H bending vibration of molecularly adsorbed water or hydrogen-bonded hydroxyl groups. This band may also receive minor contributions from aromatic C=C vibrations originating from lignin-derived phytochemicals present in rice husk. The simultaneous occurrence of the stretching band at 3332 cm^{-1} and the bending vibration at 1550 cm^{-1} confirms the existence of hydroxyl-rich compounds that participated in nanoparticle formation and stabilization. Similar observations have been reported for biosynthesized TiO_2 nanoparticles prepared using various plant extracts (Munir et al., 2019).

The absorption peak at 1274 cm^{-1} corresponds to C–O stretching vibrations, primarily arising from alcohols, phenols, esters, and ether groups present in cellulose, hemicellulose, and lignin. These oxygen-containing functional groups act as natural capping agents by coordinating with titanium species during nucleation and particle growth, thereby restricting excessive crystal growth and limiting particle aggregation.

The distinct absorption band at 1021 cm^{-1} is attributed to the O–C–O stretching vibration associated with polysaccharides and carbohydrate-derived compounds. This band indicates the presence of residual organic molecules adsorbed onto the nanoparticle surface, which may have contributed to nanoparticle stabilization during biosynthesis. Similar carbohydrate-related vibrations have been reported for plant-mediated TiO_2 nanoparticles synthesized using agricultural biomass (Yusuf, 2023).

The most significant evidence for TiO_2 formation appears in the low-frequency region. The strong absorption band at 820 cm^{-1} corresponds to Ti–O–Ti bridging vibrations, while the peak at 599 cm^{-1} is assigned to Ti–O stretching vibrations within the TiO_2 crystal lattice. These bands are characteristic fingerprints of titanium dioxide and confirm the successful formation of Ti–O bonds after calcination. Their presence further demonstrates that titanium ions were successfully converted into crystalline titanium dioxide nanoparticles. Similar Ti–O–Ti and Ti–O absorption bands within the range of 500–850 cm^{-1} have been reported for biosynthesized anatase TiO_2 nanoparticles by Bagheri et al. (2013), Mayedwa et al. (2018), and Sreeja and Ananthan (2025).

An important observation from the spectrum is the absence of a strong C–H stretching band around 2850–2950 cm^{-1}, which is commonly associated with aliphatic hydrocarbons. The disappearance of this band indicates that most organic constituents originating from the rice husk extract were removed during calcination at 500 °C, leaving only a small quantity of surface-bound phytochemicals responsible for nanoparticle stabilization. This observation confirms the effectiveness of the calcination process in improving the purity and crystallinity of the synthesized TiO_2 nanoparticles.

Generally the FTIR spectrum demonstrates that phytochemicals present in rice husk extract performed dual functions during nanoparticle synthesis. Initially, hydroxyl- and oxygen-containing biomolecules reduced the titanium precursor and promoted nanoparticle nucleation. Subsequently, these same functional groups adsorbed onto the nanoparticle surface, acting as natural stabilizing and capping agents that prevented excessive particle growth. The preservation of surface hydroxyl groups after calcination is particularly advantageous because they enhance photocatalytic activity by facilitating the formation of reactive oxygen species under ultraviolet irradiation. Consequently, the FTIR results strongly support the successful green synthesis of chemically stable TiO_2 nanoparticles possessing functional groups that are beneficial for photocatalytic degradation of pollutants, wastewater treatment, antimicrobial activity, and other environmental remediation applications.

Table 1: FTIR spectral characteristics of biosynthesized TiO_2 nanoparticles using rice husk extract

Observed Wavenumber (cm^{-1})	Relative Intensity	Typical Reference Range (cm^{-1})	Functional Group	Vibrational Assignment	Possible Source in Rice Husk	Structural/Analytical Remark
3332	Broad, Strong	3200–3600	O–H	Stretching vibration	Phenolics, alcohols, adsorbed water	Confirms hydroxyl-rich phytochemicals involved in reduction and stabilization; hydrogen-bonded surface hydroxyls beneficial for photocatalysis.
1550	Medium	1500–1650	O–H	Bending vibration	Adsorbed water, lignin derivatives	Indicates retained surface hydroxyl groups and moisture associated with biosynthesized nanoparticles.
1274	Medium	1200–1300	C–O	Stretching vibration	Alcohols, esters, lignin	Demonstrates participation of oxygen-containing phytochemicals as capping agents.
1021	Strong	1000–1100	O–C–O	Stretching vibration	Cellulose, hemicellulose, polysaccharides	Indicates carbohydrate residues that contributed to nanoparticle stabilization.
820	Medium	780–850	Ti–O–Ti	Bridging vibration	TiO_2 lattice	Confirms formation of Ti–O–Ti bonds characteristic of crystalline titanium dioxide.
599	Strong	500–700	Ti–O	Stretching vibration	TiO_2 lattice	Diagnostic band confirming successful synthesis of titanium dioxide nanoparticles.
2850–2950 *(Not observed)*	Absent	2850–2950	C–H	Stretching vibration	Aliphatic hydrocarbons	Absence indicates effective removal of most organic residues after calcination at 500 °C.

The FTIR findings are in excellent agreement with the UV–Vis analysis, which confirmed the optical characteristics of nanosized TiO_2, and with the XRD results, which verified the predominance of the crystalline anatase phase. Likewise, the SEM–EDX analysis corroborates the successful formation of titanium dioxide nanoparticles by confirming their morphology and elemental composition. Collectively, these complementary characterization techniques provide strong evidence that rice husk extract serves as an effective reducing, stabilizing, and capping agent for the environmentally benign synthesis of TiO_2 nanoparti. The findings also harmonize with previous works as shown in Table 2

Table 2: Comparison of FTIR Results with Previous Studies

Parameter	Present Study	Reported Literature	Interpretation
O–H stretching	3332 cm^{-1}	3200–3500 cm^{-1} (Srujana et al., 2022)	Excellent agreement; confirms hydroxyl-rich phytochemicals.
O–H bending	1550 cm^{-1}	1500–1650 cm^{-1} (Munir et al., 2019)	Consistent with surface-bound water and hydroxyl groups.
C–O stretching	1274 cm^{-1}	1220–1300 cm^{-1} (Yusuf, 2023)	Indicates phytochemical-mediated stabilization.
O–C–O stretching	1021 cm^{-1}	1000–1100 cm^{-1}	Typical carbohydrate vibration from biomass extracts.
Ti–O–Ti vibration	820 cm^{-1}	780–850 cm^{-1} (Bagheri et al., 2013)	Confirms TiO_2 network formation.
Ti–O vibration	599 cm^{-1}	500–700 cm^{-1} (Mayedwa et al., 2018)	Diagnostic fingerprint of crystalline TiO_2.

3.1.3 Scanning Electron Microscopy (SEM-EDX)

The surface morphology of the biosynthesized TiO_2 nanoparticles was examined using scanning electron microscopy (SEM), and the corresponding micrograph is presented in Fig. 3. The SEM image reveals that the synthesized nanoparticles are predominantly spherical to near-spherical in morphology, although considerable particle agglomeration is evident. The particles appear to be irregularly distributed, forming compact aggregates of varying sizes. Such agglomeration is a common characteristic of metal oxide nanoparticles synthesized through green routes and is primarily attributed to the high surface free energy and strong interparticle attractive forces associated with nanoscale materials. During the drying and calcination processes, individual nanoparticles tend to coalesce in order to minimize their surface energy, resulting in the formation of larger aggregates. The observed spherical morphology indicates that nucleation and crystal growth occurred uniformly during the biosynthesis process. The phytochemicals present in the rice husk extract, including phenolic compounds, flavonoids, and polysaccharides, likely acted as natural reducing and capping agents, regulating crystal growth and promoting the formation of nearly spherical particles.

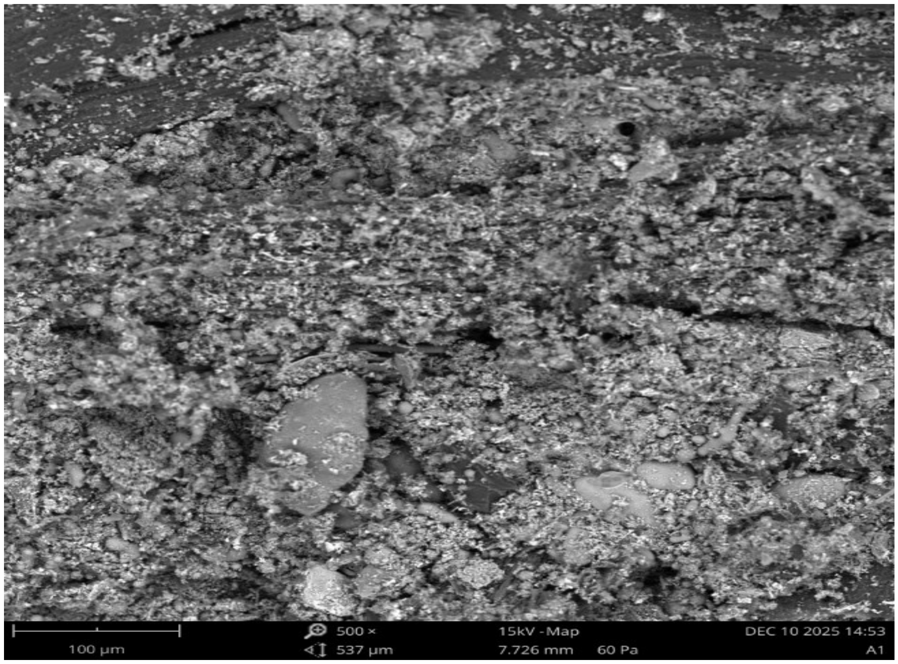

Fig. 3 SEM Image of the biosynthesized TiO_2 NPs

Nevertheless, despite the stabilizing effect of these biomolecules, complete prevention of particle aggregation was not achieved because the high-temperature calcination step (500 °C) promotes particle coalescence and neck formation between adjacent nanoparticles.

The SEM micrograph also exhibits a rough and porous surface texture, which is advantageous for adsorption and photocatalytic applications because it provides a relatively large effective surface area and numerous active sites for pollutant adsorption. The interconnected aggregates may facilitate increased contact between the catalyst surface and contaminant molecules, thereby enhancing photocatalytic degradation efficiency under ultraviolet irradiation. Similar morphological characteristics have been reported for biosynthesized TiO_2 nanoparticles prepared using plant extracts by Sreeja and Ananthan (2025), who attributed the agglomeration to the high surface energy and strong van der Waals interactions among nanosized TiO_2 particles. Likewise, Patil and Nakade (2025) reported that agglomerated spherical TiO_2 nanoparticles synthesized via green methods exhibited enhanced adsorption behaviour because of their porous aggregated structure.

Although SEM provides qualitative information regarding particle morphology, the observed aggregation makes it difficult to accurately determine the individual particle size. More precise determination of particle size distribution would require transmission electron microscopy (TEM) or dynamic light scattering (DLS). Nevertheless, the morphology observed in the present study is consistent with the UV–Vis results, which indicated nanoscale optical behaviour, and with the XRD analysis, which confirmed the formation of crystalline anatase TiO_2. Collectively, these findings demonstrate the successful synthesis of nanosized TiO_2 particles through a green route using rice husk extract.

The elemental composition of the synthesized nanoparticles was further investigated using energy-dispersive X-ray spectroscopy (EDX), and the quantitative results are summarized in Table 3. The EDX analysis indicates that the total atomic concentration of the detected elements was 100%, with titanium constituting 95.97 at.%, while the remaining elements, including vanadium (0.82 at.%), magnesium (1.18 at.%), aluminium (0.95 at.%), iron (0.74 at.%), and manganese (0.33 at.%), were present only in trace quantities. Similarly, the weight composition analysis showed that titanium accounted for 96.71 wt.%, confirming that titanium is the dominant constituent of the synthesized material.

The predominance of titanium demonstrates the successful conversion of the titanium precursor into TiO_2 nanoparticles with high elemental purity. The trace amounts of vanadium, iron, magnesium, aluminium, and manganese are likely associated with naturally occurring mineral constituents of rice husk, residual inorganic impurities, or instrumental background signals. Their concentrations are sufficiently low that they are unlikely to adversely influence the structural integrity or photocatalytic performance of the synthesized nanoparticles. Comparable titanium-rich elemental compositions have been reported for green-synthesized TiO_2 nanoparticles by Aly et al. (2025), where titanium was identified as the principal constituent of the biosynthesized material. Similarly, Jaramillo-Fierro et al. (2026) observed only trace impurity elements in rice husk-derived TiO_2-based nanomaterials, attributing these to naturally occurring minerals in the biomass precursor.

The high titanium content obtained from EDX agrees well with the XRF analysis, which showed that TiO_2 constituted 87.09% of the total oxide composition, and with the XRD results, which confirmed the formation of predominantly anatase TiO_2. Furthermore, the presence of characteristic Ti–O and Ti–O–Ti absorption bands in the FTIR spectrum provides additional evidence for the successful synthesis of titanium dioxide nanoparticles. The excellent agreement among the SEM, EDX, FTIR, XRD, and XRF analyses confirms the successful formation of chemically pure and structurally stable TiO_2 nanoparticles through the green synthesis approach.

From an application perspective, the combination of predominantly spherical morphology, rough aggregated surface, high titanium purity, and good crystallinity is expected to enhance photocatalytic performance by increasing the number of reactive surface sites available for photon absorption and pollutant interaction. These physicochemical characteristics make the biosynthesized TiO_2 nanoparticles promising candidates for photocatalytic degradation of organic pollutants, wastewater treatment, antimicrobial coatings, self-cleaning surfaces, and other environmental remediation technologies.

3.1.4 X-Ray Diffraction Analysis

The X-ray diffraction (XRD) pattern of the biosynthesized TiO_2 nanoparticles is presented in Fig. 4. The diffractogram exhibits sharp, narrow, and well-defined diffraction peaks, indicating that the synthesized material possesses a high degree of crystallinity following calcination at 500 °C. The principal diffraction peaks were observed at 2θ values of 25.39°, 27.50°, 36.16°, 41.26°, 48.05°, 53.92°, 54.37°, 56.64°, and 62.85°, corresponding to the crystallographic planes (101), (110), (103), (004), (200), (105), (211), (204), and (116), respectively.

The most intense diffraction peak occurred at 25.39°, corresponding to the (101) plane of the anatase polymorph of TiO_2. This peak agrees well with the standard diffraction pattern reported in the International Centre for Diffraction Data (ICDD) database (JCPDS Card No. 21-1272), confirming that anatase is the predominant crystalline phase. In addition, the weak diffraction peak observed at 27.50° corresponds to the (110) plane of the rutile phase according to JCPDS Card No. 21-1276 (or ICDD PDF No. 01-084-1284), indicating that a small quantity of rutile was formed during calcination.

The predominance of the anatase phase together with a minor rutile phase is highly desirable for photocatalytic applications because heterojunctions formed between the two polymorphs facilitate electron transfer, reduce electron-hole recombination, and improve photocatalytic efficiency.

Table 3: Element, Atomic concentration and Weight concentration present in the biosynthesized TiO_2 NPs from Rice Husk Extract

Atomic Number	Element	Atomic Composition (at.%)	Weight Composition (wt.%)	Possible Source	Remark
22	Ti	95.97	96.71	Titanium precursor (TTIP)	Major constituent confirming TiO_2 formation
23	V	0.82	0.88	Natural mineral impurity	Trace level; negligible effect
26	Fe	0.74	0.88	Rice husk ash/mineral residue	Minor impurity
12	Mg	1.18	0.60	Biomass mineral content	Trace element
13	Al	0.95	0.54	Rice husk silica/mineral fraction	Trace impurity
25	Mn	0.33	0.39	Natural mineral residue	Trace impurity
Total	—	100.00	100.00	—	—

Previous studies have shown that mixed anatase-rutile TiO_2 generally exhibits superior photocatalytic activity compared with either pure anatase or pure rutile owing to improved charge separation and enhanced surface reactivity (Bagheri et al., 2013; Baamer et al., 2024).

The absence of diffraction peaks corresponding to titanium hydroxide, titanium oxyhydroxide, or other crystalline impurities demonstrates that the titanium tetraisopropoxide precursor was successfully converted into crystalline titanium dioxide during the green synthesis process. Furthermore, no detectable reflections attributable to amorphous carbon or residual plant-derived compounds were observed, indicating that calcination at 500 °C effectively removed most organic constituents originating from the rice husk extract. The interplanar spacing (d-spacing) of each diffraction peak was calculated using Bragg's Law shown as equation 2 (6Eddy *et al*., 2024b)

$$n\lambda = 2dsin\theta \quad (1)$$

where, n = 1 (first-order diffraction), λ=1.5406 (Cu-Kα radiation), d = interplanar spacing (Å), and θ = Bragg angle. The calculated d-spacing values showed excellent agreement with the corresponding ICDD standard data, with deviations generally less than 0.5%, indicating high crystallographic accuracy and confirming the successful formation of tetragonal TiO_2. The sharpness of the diffraction peaks also indicates relatively large crystalline domains and low lattice distortion.

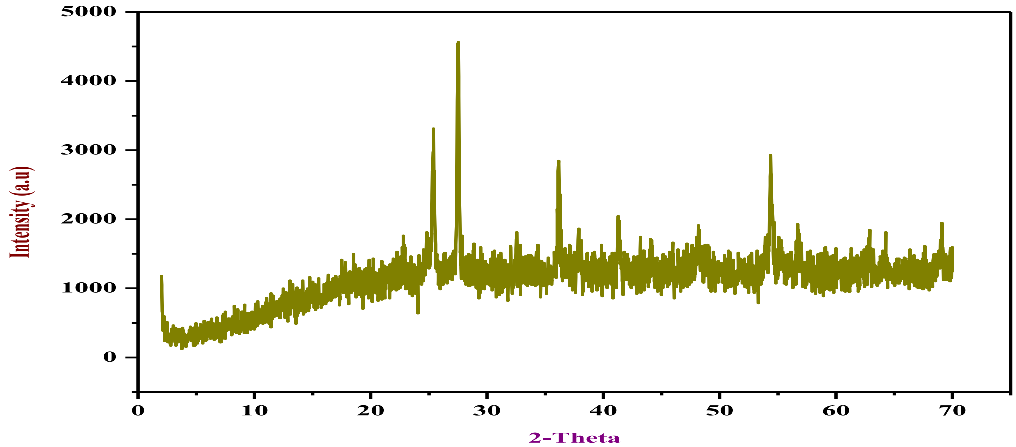

Fig. 4 XRD patterns of the biosynthesized TiO_2 NPs

Although precise crystallite size determination requires the full width at half maximum (FWHM) obtained from the original XRD raw data, the observed peak profile qualitatively suggests good crystallinity and successful crystal growth during calcination. These findings are consistent with the UV–Vis spectrum, which exhibited a characteristic absorption edge at 374 nm, and with the FTIR spectrum, where the appearance of Ti–O and Ti–O–Ti vibrations confirmed the formation of crystalline titanium dioxide. From this study, the XRD results demonstrate that the rice husk-mediated synthesis route produced highly crystalline TiO_2 nanoparticles composed predominantly of the anatase phase with a small amount of rutile. This mixed-phase composition is expected to enhance photocatalytic activity, adsorption performance, and environmental remediation efficiency through improved charge carrier separation and increased reactive surface sites.

3.1.5 X-Ray Fluorescence Analysis

The oxide composition of the biosynthesized TiO_2 nanoparticles determined by X-ray fluorescence (XRF) spectroscopy is presented in Table 5. The XRF analysis revealed that TiO_2 constituted 87.091 wt.% of the total oxide composition, confirming that titanium dioxide is the predominant crystalline oxide present in the synthesized material. The high TiO_2 concentration demonstrates the successful conversion of titanium tetraisopropoxide (TTIP) into titanium dioxide during the green synthesis process and indicates that the rice husk extract effectively facilitated the hydrolysis, nucleation, and stabilization of the nanoparticles.

Besides TiO_2, only trace quantities of other oxides were detected, including Co_3O_4 (0.2878 wt.%), V_2O_5 (0.2621 wt.%), MgO (0.1700 wt.%), SiO_2 (0.1492 wt.%), Al_2O_3 (0.0759 wt.%), CaO (0.0268 wt.%), SO_3 (0.0156 wt.%), Fe_2O_3 (0.0072 wt.%), Ta_2O_5 (0.0024 wt.%), ZnO (0.0015 wt.%), NiO (0.0006 wt.%), and Au (0.0004 wt.%). Collectively, these minor oxides account for only about 12.91 wt.% of the total composition, indicating that impurities are present only at trace levels.

The occurrence of these minor oxides is expected in plant-mediated synthesis routes because rice husk naturally contains small quantities of inorganic minerals, particularly silica, magnesium, calcium, aluminium, iron, and other trace metals.

Table 4. Crystallographic parameters of biosynthesized TiO_2 nanoparticles

Experimental 2θ (°)	Standard 2θ (°) (ICDD/JCPDS)	Crystal Plane (hkl)	d-spacing (Experimental) (Å)	Standard d-spacing (Å)	Phase	JCPDS Card No.	Observation
25.39	25.30	(101)	3.505	3.520	Anatase	21-1272	Strongest peak
27.50	27.44	(110)	3.240	3.248	Rutile	21-1276 /01-084-1284	Minor rutile phase
36.16	36.10	(103)	2.483	2.485	Anatase	21-1272	Sharp diffraction peak
41.26	41.20	(004)	2.186	2.188	Anatase	21-1272	Good crystallinity
48.05	48.05	(200)	1.891	1.892	Anatase	21-1272	Characteristic anatase peak
53.92	53.89	(105)	1.698	1.700	Anatase	21-1272	High crystallinity
54.37	54.32	(211)	1.685	1.687	Anatase	21-1272	Well-resolved peak
56.64	56.63	(204)	1.624	1.625	Anatase	21-1272	Good agreement
62.85	62.69	(116)	1.478	1.480	Anatase	21-1272	Confirms anatase structure

Among the detected impurity oxides, SiO_2 deserves particular attention because rice husk is widely recognized as a silica-rich agricultural biomass. The small SiO_2 content (0.1492 wt.%) indicates that the washing, extraction, and calcination procedures effectively minimized silica incorporation into the synthesized TiO_2 nanoparticles. This finding demonstrates that the adopted synthesis protocol produced a highly purified titanium dioxide product despite the silica-rich nature of the biomass precursor.

Similarly, the very low concentrations of Fe_2O_3, MgO, Al_2O_3, and CaO suggest that naturally occurring mineral constituents present in the rice husk were efficiently removed during the synthesis and purification stages. The trace amount of V_2O_5 detected is consistent with the EDX analysis, which identified vanadium only at very low concentrations. Such trace quantities are insufficient to modify the crystal lattice or adversely affect the photocatalytic performance of TiO_2.

The high TiO_2 purity obtained in the present study compares favourably with values reported for other green synthesis methods employing plant extracts. Supriyatna et al. (2025) similarly reported high-purity TiO_2 synthesized from low-grade ilmenite, while Sreeja and Ananthan (2025) observed that biosynthesized TiO_2 nanoparticles prepared using *Melia azedarach* leaf extract contained only trace impurity oxides after calcination. The present findings therefore confirm that rice husk extract is an efficient and environmentally sustainable precursor for producing chemically pure TiO_2 nanoparticles.

Table 5: Oxide composition of biosynthesized TiO_2 nanoparticles determined by XRF

Oxide	Chemical Formula	Composition (wt.%)	Classification	Possible Source	Remark
Titanium dioxide	TiO_2	**87.0910**	Major oxide	TTIP precursor	Dominant phase confirming successful TiO_2 synthesis
Cobalt oxide	Co_3O_4	0.2878	Trace oxide	Natural impurity/instrumental background	Negligible influence on TiO_2 properties
Vanadium pentoxide	V_2O_5	0.2621	Trace oxide	Mineral residue	Consistent with EDX results
Magnesium oxide	MgO	0.1700	Minor oxide	Rice husk mineral content	Naturally occurring biomass mineral
Silicon dioxide	SiO_2	0.1492	Minor oxide	Rice husk silica	Very low silica incorporation
Aluminium oxide	Al_2O_3	0.0759	Trace oxide	Biomass ash	Minor impurity
Calcium oxide	CaO	0.0268	Trace oxide	Plant mineral content	Negligible concentration
Sulfur trioxide	SO_3	0.0156	Trace oxide	Sulfur-containing compounds	Residual inorganic constituent
Iron(III) oxide	Fe_2O_3	0.0072	Trace oxide	Biomass minerals	Very low concentration
Tantalum pentoxide	Ta_2O_5	0.0024	Trace oxide	Instrumental/background	Negligible
Zinc oxide	ZnO	0.0015	Trace oxide	Biomass impurity	Negligible
Nickel oxide	NiO	0.0006	Trace oxide	Instrumental/background	Negligible
Gold	Au	0.0004	Trace element	Instrumental contamination/coating	Not structurally significant
Total	—	**100.0000**	—	—	—

The XRF results are in excellent agreement with the findings obtained from the other characterization techniques. The XRD analysis confirmed that the synthesized material consists predominantly of crystalline anatase TiO_2 with only a minor rutile phase, while the EDX analysis identified titanium as the dominant elemental constituent, accounting for 96.71 wt.% of the detected elements. Likewise, the FTIR spectrum exhibited characteristic Ti–O and Ti–O–Ti vibrational bands, confirming the formation of titanium dioxide, whereas the

UV–Vis spectrum demonstrated the characteristic optical absorption behaviour of nanosized TiO_2 with a band gap energy of approximately 3.32 eV. The strong agreement among these complementary analytical techniques provides convincing evidence that the synthesized nanoparticles possess high chemical purity, excellent crystallinity, and favourable physicochemical properties (Akpanudo, 2024).

From an application perspective, the high TiO_2 purity (87.091 wt.%) together with the low concentrations of secondary oxides is advantageous because impurity phases often act as recombination centres that reduce photocatalytic efficiency. The predominance of TiO_2 observed in the present study therefore suggests that the biosynthesized nanoparticles are well suited for photocatalytic degradation of organic pollutants, wastewater treatment, antimicrobial coatings, self-cleaning materials, solar energy conversion, and other environmental remediation applications.

4.0 Conclusion

The present study successfully demonstrated the green synthesis of titanium dioxide (TiO_2) nanoparticles using rice husk (*Oryza sativa*) extract as an environmentally friendly reducing and stabilizing agent. UV–Vis spectroscopy revealed a characteristic absorption maximum at 374 nm, confirming nanoparticle formation, while FTIR analysis identified hydroxyl, carbonyl, Ti–O and T-O-T functional groups that verified the involvement of phytochemicals in nanoparticle synthesis and stabilization. XRD analysis confirmed the formation of highly crystalline TiO_2 composed predominantly of the anatase phase with a minor rutile phase, indicating favourable structural characteristics for photocatalytic applications. XRF analysis further showed that TiO_2 constituted 87.091% of the total oxide composition, demonstrating high chemical purity, whereas SEM–EDX analysis revealed predominantly spherical, agglomerated nanoparticles with titanium as the major elemental constituents. Collectively, these findings confirm that rice husk extract is an effective and sustainable precursor for producing high-quality TiO_2 nanoparticles with physicochemical properties suitable for environmental remediation and related photocatalytic applications. The findings of this study provide a sustainable approach for producing TiO_2 nanoparticles from rice husk extract and establish a foundation for future investigations into their photocatalytic performance, reusability, and large-scale environmental remediation applications.

5.0 References

Akinnawo, S. (2019). Synthesis, modification, applications and challenges of titanium dioxide nanoparticles. *Research on Engineering, 3*, 10–22.

Akpanudo, N. W., & Olabemiwo, O. M. (2024a). Green synthesis and characterization of copper nanoparticles (CuNPs) and composites (CuC) using the *Echinochloa pyramidalis* extract and their application in the removal of methylene blue dye from wastewater. *Water Practice & Technology, 19*(2), 324–342.

Akpanudo, N. W., & Olabemiwo, O. M. (2024b). Synthesis and characterization of silver nanoparticles and nanocomposites using *Echinochloa pyramidalis* (Antelope grass) plant parts and the application of the nanocomposite in the removal of lead from simulated wastewater. *South African Journal of Chemical Engineering, 47*(1), 98–110.

Akpanudo, O. (2024). Pore parameters analysis of *Echinochloa pyramidalis* leaf-doped silver nanoparticles. *Communication in Physical Sciences, 11*(4), 711–720.

Alcazar, K., Tous, L., Herrera, A., Martinez-Bernett, D., & Saba, M. (2026). TiO_2 nanoparticles obtained by green synthesis: Characterization and evaluation of their effect on the self-cleaning and antifungal properties of an aqueous paint-type coating. *Nanomaterials, 16*(2), Article 91. https://doi.org/10.1007/s44509-026-00006-2

Al-Mamun, M. R., Hossain, K. T., Mondal, S., Khatun, M. A., Islam, M. S., & Khan, M. Z. H. (2022). Synthesis, characterization, and photocatalytic performance of methyl orange in aqueous TiO_2 suspension under UV and solar light irradiation. *South African Journal of Chemical Engineering, 40*, 113–125.

Aly, S. T., Farouk, S. M., Zaki, H., Tohamy, T. A., Sheikh, M. E., El, A., Sultan, R. Z., Fouda, M., Mustafa, H., Sater, O. A., Ezzat, M., & Mabrouk, M. A. (2025). Optimizing and characterization of titanium dioxide extracted from black sand using response surface methodology (RSM). https://doi.org/10.1186/s13065-025-01675-z

Aminzai, M. T., Yildirim, M., & Yabalak, E. (2024). Metallic nanoparticles unveiled: Synthesis, characterization, and their environmental, medicinal, and agricultural applications. *Talanta, 280*, 126790, DOI: 10.1016/j.talanta.2024.126790

Aravind, M., Amalanathan, M., & Mary, M. S. M. (2021). Synthesis of TiO_2 nanoparticles by chemical and green synthesis methods and their multifaceted properties. *SN Applied Sciences, 3*(4), 1–10. https://doi.org/10.1007/s42452-021-04281-5

Awad, M. A., Ortashi, K. M. O., Alenazi, W., Alfaifi, F. S., & Al-Huqail, A. A. (2025). Green synthesis of titanium dioxide nanoparticles: Characterization and evaluation of their potential for photocatalytic and dielectric applications. *Molecules, 30*(24), Article 4701. https://doi.org/10.3390/molecules30244701

Baamer, D. F., Helmy, E. T., Mostafa, M. M. M., & Pan, J. H. (2024). Synthesis of TiO_2 nanoparticles using different routes with enhanced photocatalytic and antibacterial properties. *Ceramics International, 50*, 15780–15789.

Bagheri, S., Shameli, K., & Abd Hamid, S. B. (2013). Synthesis and characterization of anatase titanium dioxide nanoparticles using egg white solution via sol–gel method. *Journal of Chemistry, 2013*, Article 848205, https://doi.org/10.1155/2013/848205

Biosci, I. J., Patil, S. B., & Nakade, D. B. (2025). Biosynthesis of TiO_2 nanoparticles using red seaweed: Detailed characterization, *6655*, 36–45.

Chen, D., Cheng, Y., Zhou, N., Chen, P., Wang, Y., Li, K., Huo, S., Cheng, P., Peng, P., Zhang, R., et al. (2020). Photocatalytic degradation of organic pollutants using TiO_2-based photocatalysts: A review. *Journal of Cleaner Production, 268*, 121725.

Eddy, N. O., Odiongenyi, A. O., Garg, R., Ukpe, R. A., Garg, R., Nemr, A. E., Ngwu, C. M., et al. (2023). Quantum and experimental investigation of the application of *Crassostrea gasar* (mangrove oyster) shell–based CaO nanoparticles as adsorbent and photocatalyst for the removal of procaine penicillin from aqueous solution. *Environmental Science and Pollution Research, 30*(23), 64036–64057.

Eddy, N. O., Jibrin, J. I., Ukpe, R. A., Odiongenyi, A., Iqbal, A., Kasiemobi, A. M., Oladele, J. O., & Runde, M. (2024a). Experimental and Theoretical Investigations of Photolytic and Photocatalysed Degradations of Crystal Violet Dye (CVD) in Water by oyster shells derived CaO nanoparticles (CaO-NP), *Journal of Hazardous Materials Advances,* 13, 100413, https://doi.org/10.1016/j.hazadv.2024.100413

Eddy, N. O., Oladede, J., Eze, I. S., Garg, R., Garg, R., & Paktin, H. (2024). Synthesis and characterization of CaO nanoparticles from periwinkle shell for the treatment of tetracycline-contaminated water by adsorption and photocatalyzed degradation. *Results in Engineering*, *103374*. https://doi.org/10.1016/j.rineng.2024.103374

Ganapathi, C. H., Ashok, K., Venkateswara, R., Shilpa, C. H., & Tambur, P. (2015). Green synthesis of TiO_2 nanoparticles using *Aloe vera* extract. *International Journal of Advanced Research in Physical Sciences, 2*, 28–34.

Jaramillo-Fierro, X., Cueva, J.-P., Ramón, J., & Valarezo, E. (2026). Rice Husk Ash Geopolymers Modified with Fe_3O_4 or $ZnTiO_3/TiO_2$ Nanoparticles for the Adsorption and Photodegradation of Organic Dyes. *Nanomaterials*, *16*(7), 413. https://doi.org/10.3390/nano16070413

Mayedwa, N., Mongwaketsi, N., Khamlich, S., Kaviyarasu, K., Matinise, N., & Maaza, M. (2018). Green synthesis of nickel oxide, palladium and palladium oxide synthesized via *Aspalathus linearis* natural extracts: Physical properties and mechanism of formation. *Applied Surface Science, 446*, 266–272.

Mittal, A. K., Chisti, Y., & Banerjee, U. C. (2013). Synthesis of metallic nanoparticles using plant extracts. *Biotechnology Advances, 31*(2), 346–356. https://doi.org/10.1016/j.biotechadv.2013.01.003

Munir, T., Sharif, M., Ali, H., Kashif, M., Sohail, A., & Sabir, N. (2019). Impact of silver dopant on structural and optical properties of TiO_2 nanoparticles. *14*(2), 279–284.

Pandey, R., & Vishwakarma, V. (2026). Green synthesis of metal-based nanoparticles using *Aloe vera* (L.) Burm.f: A review. *Discover Chemistry, 3*, Article 122. https://doi.org/10.1007/s44371-026-00527-6

Rahman, M. M., Naim, Z., Jannat, M. M., Monira, M. F., Alam, M. A., & Rahaman, M. H. (2026). Bio-engineered TiO_2 nanoparticles for circular nanocomposites: Sustainable synthesis, enhanced functional performance, and emerging applications. *Chemistry of Inorganic Materials, 9*, Article 100156. https://doi.org/10.1016/j.cinorg.2026.100156

Sety, N. K., Zeenat, A., Pradeep, K. M., & Pradeep, K. (2020). Green synthesis of TiO_2 nanoparticles from *Syzygium cumini* extract for photo-catalytic removal of lead (Pb) in explosive industrial wastewater. *Green Processing and Synthesis, 9*, 171–181.https://doi.org/10.1515/gps-2020-0018

Shakeel, N., Piwoński, I., Iqbal, P., & Kisielewska, A. (2025). Green synthesis of titanium dioxide nanoparticles: Physicochemical characterization and applications: A review. *International Journal of Molecular Sciences, 26*(12), 5454. https://doi.org/10.3390/ijms26125454

Souza França, Y. K., Pereira, K. S., Feitosa, Y. H. C., Marques, V. B., & de Souza, D. R. (2025). Titanium dioxide (TiO_2) and photocatalysis: A detailed overview of the synthesis, applications, challenges, advances and prospects for sustainable development. *Orbital: The Electronic Journal of Chemistry, 17*, 355–381.

Sreeja, P., & Ananthan, M. R. (2025). Green synthesis of titanium dioxide nanoparticles using *Melia azedarach* leaf extract and evaluation. *26*(3), 370–379.

Srikar, S., Giri, D., Pal, D., Mishra, P., & Upadhyay, S. (2016). Green synthesis of silver nanoparticles: A review. *Green and Sustainable Chemistry, 6*, 34–56. https://doi.org/10.4236/gsc.2016.61004

Srujana, S., Anjamma, M., Singh, B., Dhakar, R. C., Natarajan, S., & Hechhu, R. (2022). A comprehensive study on the synthesis and characterization of TiO_2 nanoparticles using *Aloe vera* plant extract and their photocatalytic activity against MB dye. *Research Article*, 2022, https://doi.org/10.1155/2022/7244006

Supriyatna, Y. I., Astuti, W., Sumardi, S., Prasetya, A., Ginting, L. I. B., Wahab, W., & Petrus, H. T. B. M. (2025). Titanium dioxide production from low-grade ilmenite ore: Mineral characterisation and optimization. *70*, 77–86.

Syamsol Bahri, S., Harun, Z., Khadijah Hubadillah, S., Norhayati Wan Salleh, W., Rosman, N., Hasliza Kamaruddin, N., Hafeez Azhar, F., Sazali, N., Adiba Raja Ahmad, R., & Basri, H. (2021). Review on recent advance biosynthesis of TiO_2 nanoparticles from plant-mediated materials: Characterization, mechanism and application. *IOP Conference Series: Materials Science and Engineering, 1142*(1), 012005. https://doi.org/10.1088/1757-899X/1142/1/012005

Syed, S. M., Kulkarni, S., Patil, M., & Satpute, K. (2026). A comprehensive review of green synthesis methods and applications of nanoparticles derived from plant extracts and microorganisms. *Discover Green Chemistry, 1*, Article 6. https://doi.org/10.1007/s44509-026-00006-2

Yusuf, M. O. (2023). Bond Characterization in Cementitious Material Binders Using Fourier-Transform Infrared Spectroscopy. *Applied Sciences*, *13*(5), 3353. https://doi.org/10.3390/app13053353

Declaration

Ethics Approval and Consent to Participate

Not applicable

Consent for Publication

All authors have read and approved the final version of the manuscript and consented to its publication.

Availability of Data and Materials

Data shall be made available upon request

Funding

The author declared no source of funding

Competing Interests

The authors declare that they have no known competing financial interests or personal relationships that could have influenced the work reported in this paper.

Author Contributions

M.S. conceived the study, conducted the experimental work, analyzed the data, and drafted the manuscript. O.O.J. supervised the research, contributed to experimental design, interpreted the characterization results, and critically revised the manuscript. A.H. assisted with data validation, literature review, statistical interpretation, manuscript editing, and approved the final version for publication.